ELSEVIER

Journal of Nuclear Materials 252 (1998) 150–155

journal of nuclear materials

Thermal transport in CKC TiB_2-doped graphite

J.W. Davis, A.A. Haasz *

Fusion Research Group, University of Toronto Institute for Aerospace Studies, 4925 Dufferin St., North York, Ont., Canada M3H 5T6

Received 14 March 1997; accepted 22 August 1997

Abstract

The thermal diffusivity and heat capacity of TiB_2-doped graphites (fabricated by Ceramics Kingston Ceramique, Canada) have been measured in the temperature range 300 to 1000 K, using the laser flash technique; from these data, the thermal conductivities have been calculated. The specimens were found to be highly anisotropic vis a vis thermal diffusivity/conductivity. For the high thermal flow direction, the thermal conductivity was reduced by a factor of 1.4–2.3 for the TiB_2-doped specimens as compared to the undoped material, resulting in values about the same as for EK98 (Ringsdorff, Germany). In the low thermal flow direction, the thermal conductivity of the material with 20% TiB_2 was increased as compared to the undoped specimen, while the material with 10% TiB_2 was about the same. © 1998 Elsevier Science B.V.

1. Introduction

Carbon-based materials are considered primary candidates for certain plasma-facing components in present and future magnetic fusion reactors. There is, however, major concern with regard to the erosion characteristics of carbon when exposed to hydrogen- and oxygen-containing plasmas. In a previous series of experiments with doped graphites, we compared the thermal [1], erosion [2,3] and hydrogen retention characteristics [4] of graphites containing B, Si, Ti, Ni and W. From these materials, we have identified B and Ti as being the most effective in the reduction of erosion. In particular, chemical erosion due to 1 keV H^+ impact was reduced by up to a factor of 5 with the addition of B [2], and radiation-enhanced sublimation could be nearly completely suppressed by the addition of Ti [3]. In the current experiments, we have extended our previous work, by considering materials containing both of these dopants, in the form of TiB_2.

The first part of this new study, which is reported here, concerns the thermal transport properties of these materials. Test specimens containing 0, 10 and 20% TiB_2 were fabricated by Ceramics Kingston Ceramique (CKC) from finely ground pyrolytic graphite (< 1 μm) mixed with sub-μm TiB_2 powder and an organic binder. Specimen blocks were prepared with a final heating stage at ~ 2270 K. The TiB_2 concentrations are nominal values provided by the manufacturer based on the molecular concentration of TiB_2 (N_{TiB_2}) and the atomic concentration of C (N_C), i.e. $N_{TiB_2}/(N_{TiB_2} + N_C) \sim 0.1$ or 0.2. A more extensive characterization of the specimens will be performed in conjunction with ongoing erosion and hydrogen retention experiments.

2. Experiment

Thermal diffusivities and heat capacities were measured using the laser flash technique. All experiments were performed with the apparatus and procedures of Ref. [1]. Specimen temperatures were measured using chromel–alumel thermocouples (13 and 25 μm diameter) which were bonded to the back face of the specimens with a graphite epoxy. Specimens were heated to temperatures up to 1000 K in a vacuum oven by radiation from nearby tungsten filaments. Further details of the facility and procedures are given in Refs. [1,5].

The thermal diffusivity (α) is obtained from the time required to reach 1/2 of the total temperature rise on the

* Corresponding author. Fax: +1-416 667 7743; e-mail: aahaasz@utias.utornoto.ca.

PII S0022-3115(97)00287-0

back face of the specimen due to a laser pulse impacting on the front face [6]:

$$\alpha = \frac{1.38L^2}{\pi^2 t_{1/2}} \tag{1}$$

where L = specimen thickness; $t_{1/2}$ = time to reach 1/2 of the total temperature rise.

The effective specimen temperature for the thermal diffusivity measurement is [6]:

$$T_{\text{eff}} = T_{\text{initial}} + 1.6\Delta T \tag{2}$$

where ΔT is the total temperature rise. The method of Heckman [7] was used to make corrections for the finite laser pulse time effect. For the range of temperatures of the present experiments, corrections for radiation losses from the heated face of the specimen were not required [5].

The diffusivity measurement, therefore involves primarily the knowledge of the laser firing time and the time at which the back face temperature has reached 1/2 of its maximum value. The shape of the initial temperature rise, as well as the longer cooling curves of the temperature transients may be used to determine the specimen cooling rate or the presence of undesired radial heat transport. The laser energy was chosen to produce a temperature rise on the order of 5 K to provide good signal resolution, while minimizing surface effects, such as ablation.

The heat capacity (C_p) of a specimen may also be measured by the pulsed laser technique, according to:

$$C_p = \frac{\eta Q}{\rho L \Delta T} \tag{3}$$

where η = energy absorption efficiency; Q = laser beam energy density and ρ = specimen density.

The effective temperature used in the specific heat calculation is:

$$T_{\text{eff}} = T_{\text{initial}} + 0.5\Delta T \tag{4}$$

The total temperature rise, ΔT, is available as part of the diffusivity measurement as discussed above. The only unknown quantity remaining in Eq. (3) is η, the fractional amount of incident laser energy absorbed by the specimen.

As found in our previous study of CKC-produced doped graphites [1], the current specimens are also highly anisotropic. In accordance with our previous description [2–4], the direction of high thermal conductivity is referred to as the 'edge' orientation, while the direction of low thermal conductivity is referred to as the 'base' orientation. Specimen dimensions were ~ 9 mm diameter by ~ 3 mm thick for the base-oriented specimens and ~ 9 mm diameter by ~ 5 mm thick for the edge-oriented specimens.

In all calculations, room temperature values are used

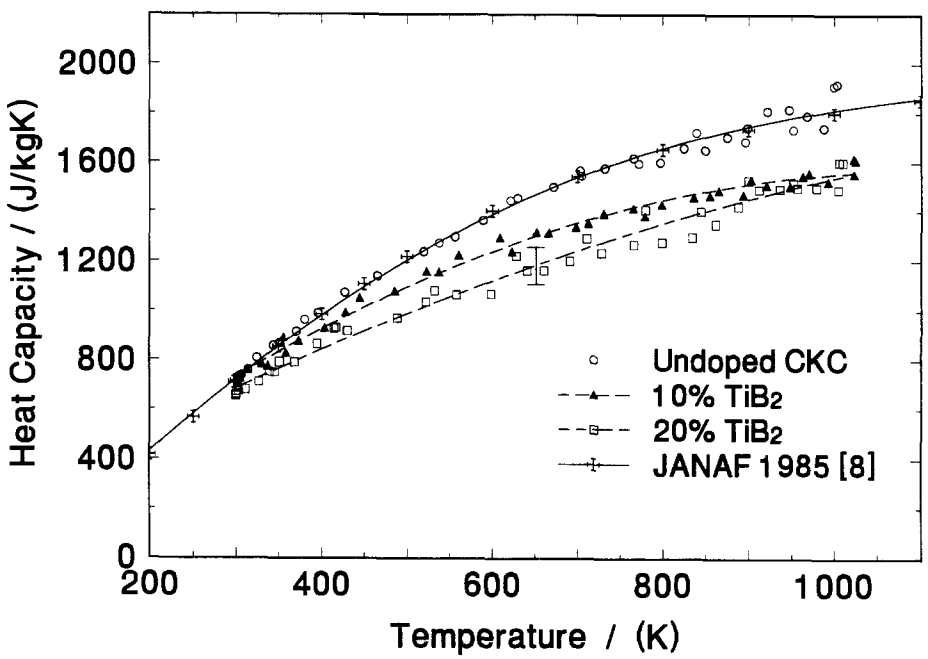

Fig. 1. Heat capacity measurements obtained for the edge orientation of the undoped CKC and TiB_2-doped graphites, assuming a laser energy absorption coefficient of $\eta = 0.585$. The solid line is a 5th order polynomial fit to literature values for graphite [8] and the broken lines through the TiB_2-doped graphite data are the 2nd order polynomial fits used in the calculation of thermal conductivity in Figs Fig. 2b and Fig. 3b). Coefficients for the 2nd-order polynomial fits are provided in Table 1. The representative error bar shown are estimated from the data scatter and a consideration of the errors described in Section 2. (The TiB_2 concentrations are nominal values provided by the manufacturer based on the molecular concentration of TiB_2 (N_{TiB_2}) and the atomic concentration of C (N_C), i.e. $N_{TiB_2}/(N_{TiB_2} + N_C) \sim 0.1$ or 0.2.)

for the density, ρ, and the thickness, L. Over the temperature range of the study, the upper limit on the thermal expansion is that corresponding to the 'c'-direction (across the planes) of single crystal graphite, or $\sim 2\%$ at 1000 K [10]. (In the 'ab'-direction, thermal expansion is more than an order of magnitude smaller.) This would introduce errors $< 4\%$ in the diffusivity (base orientation only) and $< 2\%$ in the conductivity. The thermal expansion of com-

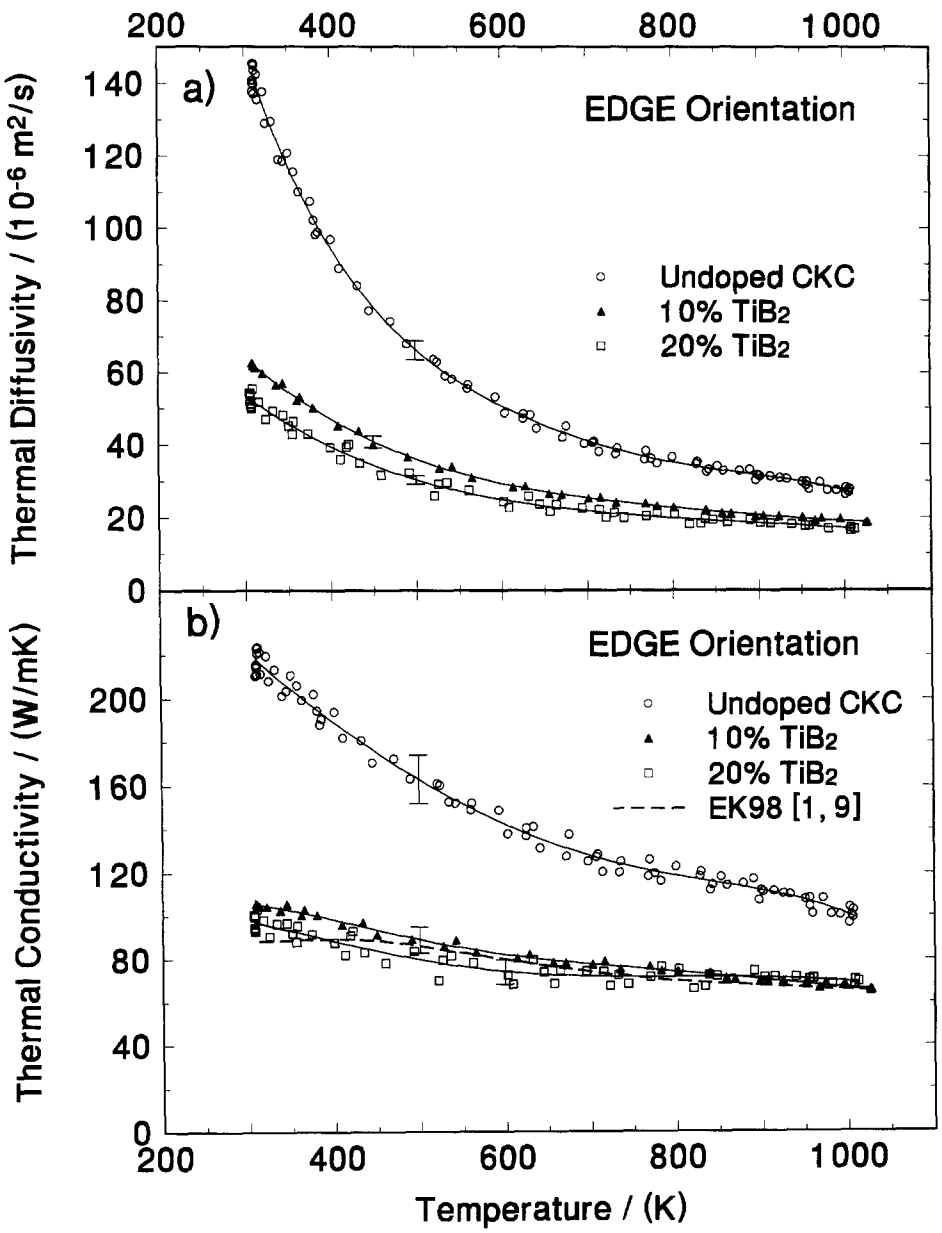

Fig. 2. (a) Thermal diffusivity for the edge orientation of the undoped CKC and TiB_2-doped graphites: The lines drawn through the data are 5th order polynomial fits. (b) Thermal conductivity values (edge orientation) calculated from the data in (a) and the curves fit to the data in Fig. 1, using Eq. (5). Thermal conductivity results of EK98 [1,9] are shown for comparison. Coefficients for the 5th-order polynomial fits for both the diffusivity and conductivity are provided in Table 1. The representative error bars shown are estimated from the data scatter, and a consideration of the errors described in Section 2.

pression-molded graphites depends strongly on the manufacturing conditions, but is generally 3–10 times smaller [10]. Thus it is anticipated that errors $< 1\%$ are involved in the present study.

The largest sources of error in the experiment are thought to be the assumptions involved in the choice of η (5%) and measurement reproducibility (scatter). Errors in measuring the energy flux are absorbed in the η parameter. Systematic errors in measuring diffusivity are checked by taking measurements with the specimen both increasing and decreasing in temperature. Errors in the measurement of temperature and physical parameters are $< 1\%$.

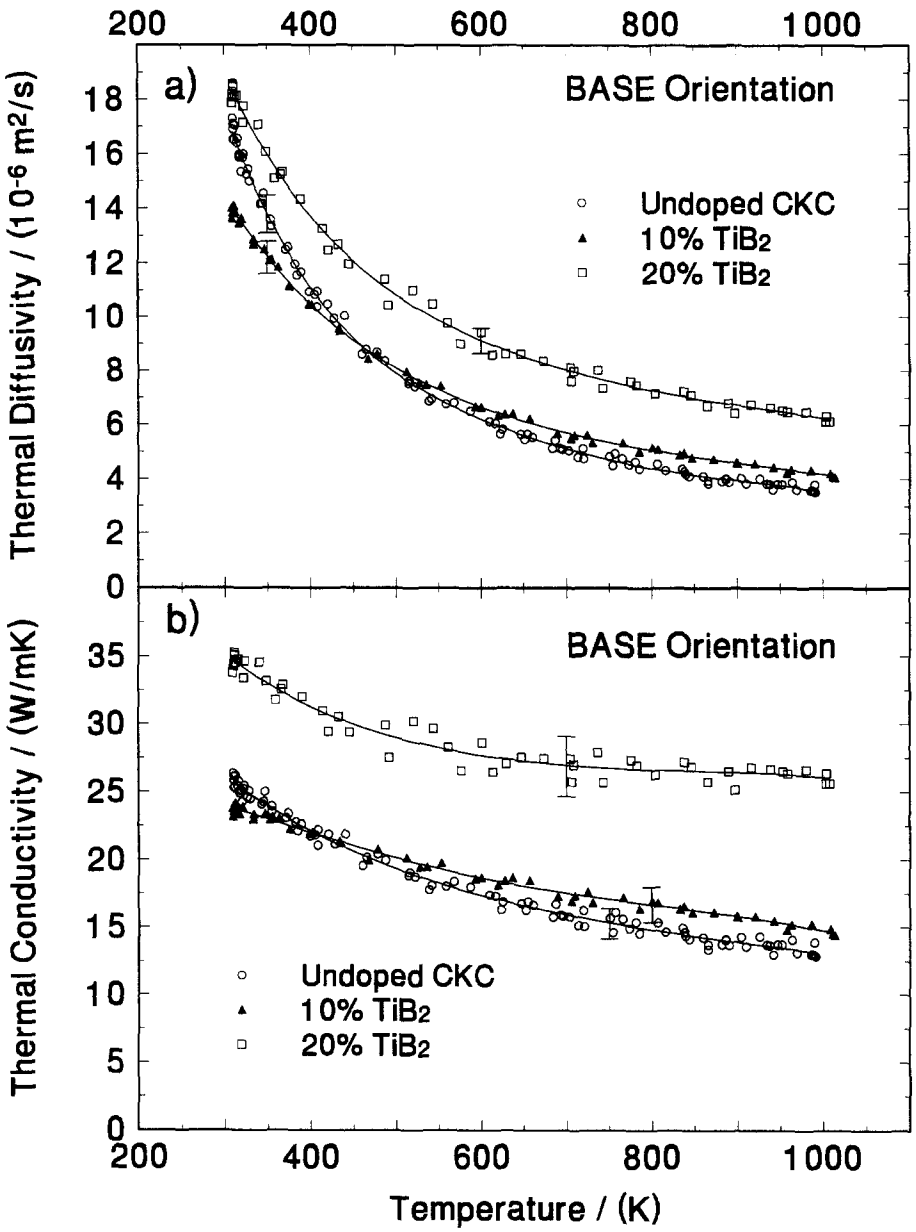

Fig. 3. (a) Thermal diffusivity for the base orientation of the undoped CKC and TiB_2-doped graphites: The lines drawn through the data are 5th order polynomial fits. (b) Thermal conductivity values (base orientation) calculated from the data in (a) and the curves fit to the data in Fig. 1, using Eq. (5). Coefficients for the 5th-order polynomial fits for both the diffusivity and conductivity are provided in Table 1. The representative error bars shown are estimated from the data scatter. and a consideration of the errors described in Section 2.

3. Results

3.1. Heat capacity

Determination of the heat capacity requires knowledge of the laser energy absorption factor, η. In the present experiment, η was obtained by comparing heat capacity measurements on the undoped specimens with literature values for graphite [8]. Measurements on the edge specimens were generally more reliable than for the base specimens for temperatures > 800 K and thus only these values are used. The value of η used, $\eta = 0.585$, is almost identical to that used in Ref. [1] ($\eta = 0.58$).

The heat capacity measurements for the edge oriented specimens are shown in Fig. 1. For the undoped CKC specimen, the data are plotted along with the literature values from Ref. [8]; the good agreement supports our choice of η. The 10 and 20% specimens are shown with the second-order polynomial fits used in the calculation of thermal conductivity; see below. There is a general decrease in C_p with the added TiB_2, however, the increase in density compensates, such that the product ρC_p is not greatly altered. Again, the results are qualitatively similar to our previous measurements for a different set of CKC-doped graphites [1].

Coefficients of the polynomial fits shown in Figs. 1–3 are given in Table 1, along with an indication of the goodness of fit.

3.2. Thermal diffusivity

The experimentally-measured thermal diffusivities for the edge and base orientations are shown in Fig. 2a and Fig. 3a, respectively. Generally, several experiments were run for each specimen and there was very good consistency independent of whether the temperature was increasing or decreasing and from run to run.

For the undoped CKC specimen, edge (Fig. 2a) thermal diffusivity values start as high as 145×10^{-6} m^2/s at room temperature, decreasing to 30×10^{-6} m^2/s at 1000 K. Undoped CKC base (Fig. 3a) orientation values follow a very similar trend, but are lower by a factor of ~ 8. The diffusivities for the doped graphites show a somewhat weaker temperature dependence, and the edge-specimen (Fig. 2a) diffusivities were lower by a factor of 2–3 as compared to the undoped CKC material. In the base direction (Fig. 3a), diffusivity values for the 10% TiB_2 material are similar to the undoped CKC base specimen, while the 20% TiB_2 material has a diffusivity up to two times higher. For this latter material, the diffusivities in the base and edge directions differ by about a factor of three.

The results are qualitatively very similar to those found for the previous series of CKC specimens [1]; the most noticeable difference is an increase of 30–50% in the diffusivity of all the edge-oriented (high-direction) specimens at 1000 K, as compared to the following specimens

Table 1
Coefficients for the polynomial fits to the heat capacity, thermal diffusivity and thermal conductivity data shown in Figs. 1–3

	Reference, $\rho = 2.025$				10% TiB_2, $\rho = 2.261$				20% TiB_2, $\rho = 2.684$			
	C_p (J/kgK)	edge		base	C_p (J/kgK)	edge		base	C_p (J/kgK)	edge		base
		α (10^{-6} m^2/s)	k (W/mK)	α (10^{-6} m^2/s)		α (10^{-6} m^2/s)	k (W/mK)	α (10^{-6} m^2/s)		α (10^{-6} m^2/s)	k (W/mK)	α (10^{-6} m^2/s)	k (W/mK)
Coefficients of polynomial fits: $A + B \cdot T + C \cdot T^2 + D \cdot T^3 + E \cdot T^4 + F \cdot T^5$													
A	−168	783	394	100	−6.63	164	−3.44	48.5	145	140	59.5	73.7	75.7
B	3.46	−4.27	−0.944	−0.569	2.84	−0.470	1.13	−0.207	1.97	−0.425	0.533	−0.357	−0.265
C	−1.47e−3	1.06e−2	1.95e−3	1.44e−3	2.69e−4	−1.28e−3	4.64e−4	−4.12e−3	4.36e−4	−1.78e−4	−5.78e−4	5.18e−4	−2.20e−3	8.43e−4	6.34e−4
D	−	−1.39e−5	−3.25e−6	−1.90e−6	−2.78e−7	−	1.40e−7	6.55e−6	−4.99e−7	2.82e−7	−	−1.79e−7	3.47e−6	−1.06e−6	−8.31e−7
E	−	9.29e−9	3.11e−9	1.27e−9	1.56e−10	−	−4.54e−10	−4.88e−9	3.00e−10	−1.86e−10	−	−9.31e−11	−2.41e−9	6.80e−10	5.77e−10
F	−	−2.52e−12	1.17e−12	−3.38e−13	3.75e−14	−	1.92e−13	1.39e−12	7.50e−14	4.26e−14	−	5.66e−14	6.09e−13	−1.77e−13	−1.66e−13
Goodness of fit parameters													
Standard deviation	37	1.9	3.9	0.20	0.43	26	0.54	1.3	0.13	0.30	4.3	1.5	3.6	0.29	0.78
Adjusted R^2	0.99164	0.99793	0.99175	0.99829	0.99058	0.99282	0.99884	0.99146	0.99878	0.99133	0.9813	0.98767	0.89603	0.99582	0.94565

studied in Ref. [1]: high-direction reference, high-direction 10% and 20% B-doped graphites and high direction 8% and 16% Ti-doped graphites.

3.3. Thermal conductivity

The thermal conductivity (k) can be found from measurements of diffusivity (α) and heat capacity (C_p) through the formula:

$$k = \rho \alpha C_p, \tag{5}$$

Plots of the thermal conductivities, which are formed by using the data points for the diffusivity, with the polynomial fits to the heat capacity, are shown in Fig. 2b and Fig. 3b for the edge and base orientations, respectively. (Data points from both diffusivity and heat capacity measurements cannot be used together, since the effective temperatures for the two measurements are different.) The general trends as observed in the thermal diffusivities are also observed for the thermal conductivity. At room temperature, the conductivity of the edge TiB_2-doped specimens are reduced by about a factor of 2, while at 1000 K, the reduction is only $\sim 30\%$. Data for the isotropic graphite EK98 (Ringsdorff, Germany) are shown on Fig. 2b for comparison [1,9]. The data fall right on top of the doped graphite results. In the base direction, the thermal conductivity of the 20% TiB_2 material is increased by about 35% at room temperature and a factor of 2 at 1000 K. The 10% TiB_2 material has a similar thermal conductivity to the Undoped CKC material in the base orientation. For both the edge and base orientations, the temperature dependence of the doped materials is weaker than for the undoped ones.

4. Summary

The thermal transport properties of TiB_2-doped graphites have been measured by the laser flash technique. In the direction of high thermal conductivity (edge orientation), the addition of the dopants tends to reduce the thermal conductivity, while in the direction of low thermal conductivity (base orientation), the dopants lead to an increase in thermal conductivity. At low temperatures, the results for both doped and undoped materials are similar in magnitude to those obtained previously for single dopants [1], while at high temperatures, the new results show thermal conductivities 30–50% higher than the Ref. [1] values. The thermal conductivity of the TiB_2-doped materials in the edge orientation is essentially the same as that for EK98 (isotropic fine grain graphite manufactured by Ringsdorff, Germany), see Fig. 2b.

Acknowledgements

This work was supported by the Canadian Fusion Fuels Technology Project. We thank Ceramics Kingston Ceramique for supplying the TiB_2-doped graphite and Charles Perez for preparing the specimens.

References

[1] B.N. Enweani, J.W. Davis, A.A. Haasz, Thermal diffusivity/conductivity of doped graphites, J. Nucl. Mater. 224 (1995) 245.
[2] A.Y.K. Chen, A.A. Haasz, J.W. Davis, Comparison of the chemical erosion yields of doped graphites, J. Nucl. Mater. 227 (1995) 66.
[3] P. Franzen, A.A. Haasz, J.W. Davis, Radiation-enhanced sublimation of doped graphites, J. Nucl. Mater. 226 (1995) 15.
[4] A.A. Haasz, J.W. Davis, Deuterium retention in doped graphites, J. Nucl. Mater. 232 (1996) 219.
[5] B.N. Enweani, M.A. Sc. thesis, University of Toronto Institute for Aerospace Studies, 1994.
[6] W.J. Parker, R.J. Jenkens, C.P. Buttler, G.L. Abbott, Flash method of determining thermal diffusivity, heat capacity and thermal conductivity, J. Appl. Phys. 32 (1961) 1679–1684.
[7] R.C. Heckman, Finite pulse-time and heat-loss effects in pulse thermal diffusivity measurements, J. Appl. Phys. 44 (1973) 1455–1460.
[8] M.W. Chase Jr., et al. JANAF Thermochemical Tables, 3rd ed., 1985. J. Phys. Chem. Ref. Data 14 (Suppl. 1) (1985).
[9] E.P. Roth, R.D. Watson, M. Moss, W.D. Drotning, Thermophysical properties of advanced carbon materials for tokamak limiters, Sandia National Laboratories Report No. SAND88-2057, April 1989.
[10] H.O. Pierson, Handbook of Carbon, Graphite, Diamond and Fullerenes, Noyes Publications, Park Ridge, NJ, 1993.